ELSEVIER

PII: S0032-3861(97)00312-1

Polymer Vol. 39 No. 3, pp. 675–680, 1998

0032-3861/97/$17.00+0.00

A fracture mechanics approach to environmental stress cracking in poly(ethyleneterephthalate)

Eric J. Moskala*
Eastman Chemical Company, PO Box 1972, Kingsport, TN 37662, USA
(Received 31 January 1997; revised 3 July 1997)

Environmental stress cracking of amorphous poly(ethylene terephthalate) in aqueous sodium hydroxide was studied by using a fracture mechanics approach. Compact tension specimens were machined from injection-molded plaques and used to determine creep crack growth rate as a function of applied stress intensity factor. The effects of caustic concentration and polymer molecular weight on creep crack growth behaviour were determined. Fractographic analysis of the fracture surfaces showed that crack growth proceeded by the formation of novel discontinuous growth bands. The structure and mechanism of formation of these bands are discussed. © 1997 Published by Elsevier Science Ltd.

(Keywords: crazing; static fatigue; stress intensity factor)

INTRODUCTION

Environmental stress cracking refers to crazing and cracking that occurs when a polymer, under tension, is exposed to an aggressive chemical environment. The chemical reagent may cause crazing either by swelling the polymer or by chemically reacting with the polymer. The former mechanism has been the subject of numerous investigations and is commonly recognized as the primary cause of the majority of chemically induced failures in polymers[1–4]. However, some chemicals can initiate crazes by chemically reacting with the polymer. For example, it is well know that poly(ethylene terephthalate) (PET) can be hydrolysed by aqueous sodium hydroxide[5]. The concomitant reduction in polymer molecular weight from hydrolysis can lead to crazing and eventual catastrophic failure. Note that little, if any, polymer swelling occurs by this latter mechanism.

Environmental stress cracking of amorphous PET is a particular nuisance when the resin is used for carbonated beverage containers. The carbonation pressure coupled with the rather intricate, stress-concentrating designs of many one-piece footed containers create a potential for catastrophic failure if the container is exposed to an aggressive chemical environment. It was determined recently that field failures of these containers are consistent with alkaline-induced environmental stress cracking[6]. The source of alkalinity may stem from the various line lubricants used in container filling lines to the numerous cleaning agents that the containers may come in contact with in grocery stores or in the home.

Catastrophic failure caused by environmental stress cracking can be considered as a two-step process: initiation of a crack followed by propagation of the crack to failure. Crack initiation often occurs at flaws or defects such as contaminants, impurities, shrinkage voids and machining marks. Consequently, crack initiation is a more random process and is difficult to quantify through experimental means. Crack propagation, however, can be easily studied by using fracture mechanics. In this approach, the rate of crack propagation (da/dt) is monitored as a function of stress intensity factor (K). The stress intensity factor is a measure of the stress amplification at the crack tip and is a function of the applied loading and the geometry of the structure in which the crack is located. For a crack growing in a slow, stable manner, the relationship between da/dt and K is often expressed by

$$da/dt = AK^m \quad (1)$$

where A and m are constants which depend on material properties and test conditions[7]. The objective of this study was to use this approach to evaluate the effect of caustic concentration and polymer molecular weight on crack growth rate in PET.

EXPERIMENTAL

Compact tension specimens were machined from 3.2-mm thick injection molded plaques. Two specimens were obtained from each plaque, as shown in *Figure 1*. The specimen width (W), defined as the distance from the centre of the loading pin holes to the back face of the specimen, was equal to 50.8 mm for all specimens used in this work. Each specimen was notched with a band saw. The notch root was subsequently sharpened with a razor blade. The notch or crack length (a) is defined as the distance from the centre of the loading pin holes to the tip of the notch. The initial notch length was typically between 18 and 20 mm. All specimens were notched along the mold-flow direction.

A schematic of the rig used for the crack growth tests is shown in *Figure 2*. Typical loads ranged from 22 to 44 N. Load-line displacement was measured to the nearest micrometer with a Mitutoyo Digimatic Indicator. Crack length was determined from load-line displacement by the

* To whom correspondence should be addressed

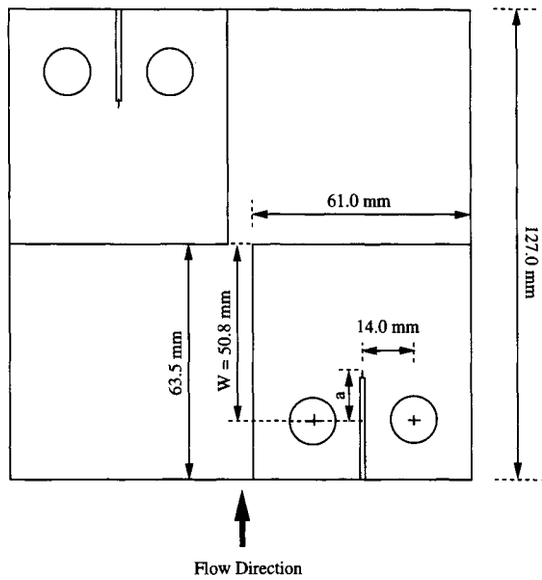

Figure 1 Diagram of compact tension specimens as machined from injection-molded plaques

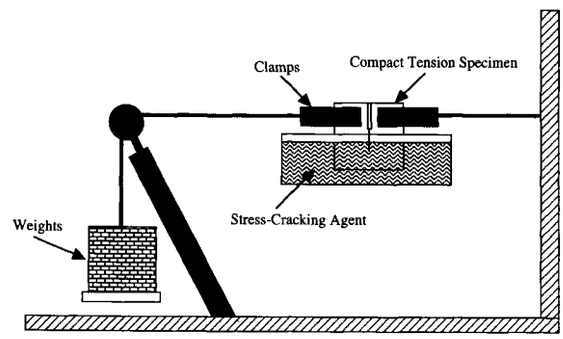

Figure 2 Schematic of rig used to determine creep crack growth rates

following relationship[8]:

$$\frac{a}{w} = 1.0002 - 4.0632u_x + 11.242u_x^2 - 106.04u_x^3 + 464.33u_x^4 - 650.68u_x^5 \quad (2)$$

The quantity u_x is given by

$$u_x = \left[\sqrt{\frac{BEV}{P}} + 1\right]^{-1} \quad (3)$$

where B is specimen thickness, E is tensile modulus, P is load and V is displacement.

The stress intensity factor (K) for mode I loading of a compact tension is given as

$$K = f\left(\frac{a}{W}\right)\left(\frac{P}{BW^{1/2}}\right) \quad (4)$$

where

$$f\left(\frac{a}{W}\right) = \left(\frac{2 + \frac{a}{W}}{\left(1 - \frac{a}{W}\right)^{3/2}}\right)\left[0.886 + 4.64\left(\frac{a}{W}\right) - 13.32\left(\frac{a}{W}\right)^2 + 14.72\left(\frac{a}{W}\right)^3 - 5.6\left(\frac{a}{W}\right)^4\right] \quad (5)$$

Crack growth rate (da/dt) was calculated by using the secant and seven-point incremental polynomial methods described in ASTM Standard E647. Each set of creep crack growth data shown in this work was recorded from one specimen only. Repeat experiments gave values of da/dt at any particular value of K that agreed to within ± 20%.

The stress cracking agent used in all tests was an aqueous solution of analytical reagent grade sodium hydroxide (caustic). All solutions were prepared with distilled water. Concentrations are expressed as weight to weight percentages. All crack growth tests were performed at ambient conditions.

The PET resins used in this study were supplied by Eastman Chemical Company, Kingsport, TN. Inherent viscosity (IV) of the injection-molded resins ranged from 0.58 to 0.88 dl g^{-1}. IV was measured in a 60/40 phenol/tetrachloroethane mixture at 23°C. Tensile modulus and yield stress values for the resins were measured according to ASTM Standard D638 by using a strain rate of 1 min^{-1}. Fractographic analyses were performed on a Wild M400 optical microscope.

RESULTS AND DISCUSSION

A plot of crack length *versus* time for PET (IV = 0.71 dl g^{-1}) in 1% caustic is shown in *Figure 3*(a). The crack accelerates as it grows, with most of the crack growth occurring during the latter part of the test. The portion of data highlighted by a box in *Figure 3*(a) is enlarged in the plot shown in *Figure 3*(b). In this expanded plot, it is evident from the distinct clustering of data that crack growth occurs

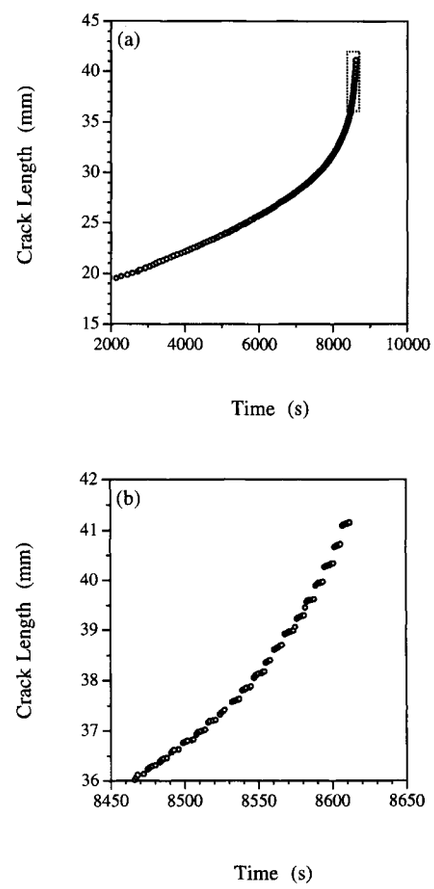

Figure 3 Crack length *versus* time for PET in 1% caustic at (a) full scale, and (b) expanded scale

in a discontinuous or stepwise manner. This hypothesis is verified by an examination of the specimen's fracture surface. *Figure 4* shows an optical micrograph of the portion of the fracture surface that coincides with the data plotted in *Figure 3*(b). Each band in the micrograph corresponds exactly to a cluster of data from the plot in *Figure 3*(b).

A possible mechanism for the formation of these discontinuous growth bands is presented in *Figure 5*. At the tip of a newly formed crack (a_1) a craze begins to grow. Extension of the craze results in an apparent increase in crack length, as determined by equations (2) and (3), although the actual crack tip is stationary. Since a typical craze is approximately 50% polymer by volume, the length of the craze is about twice the amount of apparent crack growth[9]. During extension of the craze, the caustic aggressively attacks the craze fibrils at the crack tip. After the crazed region is sufficiently damaged by hydrolysis, the crack jumps through the craze and is arrested when it reaches virgin polymer (a_2). The process repeats itself until, at some long crack length (i.e. high stress intensity factor), the energy released during the jump is sufficient to result in catastrophic failure. A somewhat analogous mechanism of crack propagation was observed by Lu and Brown[10] in a study of polyethylene under constant load in the absence of an aggressive chemical environment. According to Lu and Brown, crack initiation occurred because the craze fibrils were weakened by a process of chain disentanglement.

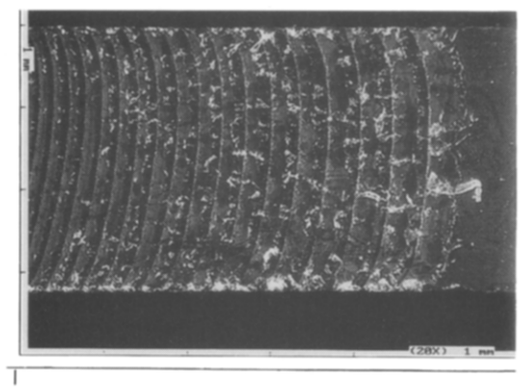

Figure 4 Optical micrograph of discontinuous growth bands on fracture surface of PET in 1% caustic. Crack growth occurs from left to right

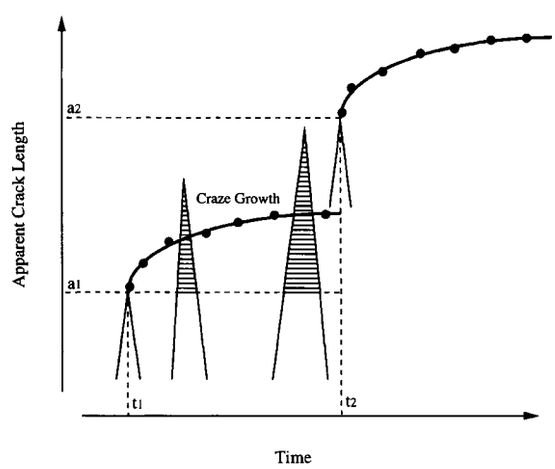

Figure 5 Schematic of relationship between craze growth and apparent crack length

Crack growth rates were determined from *Figure 3*(a) by using a secant method and are plotted *versus* stress intensity factor in *Figure 6*(a). The plot is fairly linear on a log–log scale, as predicted by equation (1). The portion of data highlighted by a box in *Figure 6*(a) corresponds to the highlighted crack length values in *Figure 3*(a) and is enlarged in the plot shown in *Figure 6*(b). In this plot, consecutive data points are connected to facilitate interpretation. Notice the periodic undulations in da/dt with increasing K. According to the crack growth mechanism described above, a high value of da/dt occurs when the crack jumps through a damaged craze zone. The subsequent

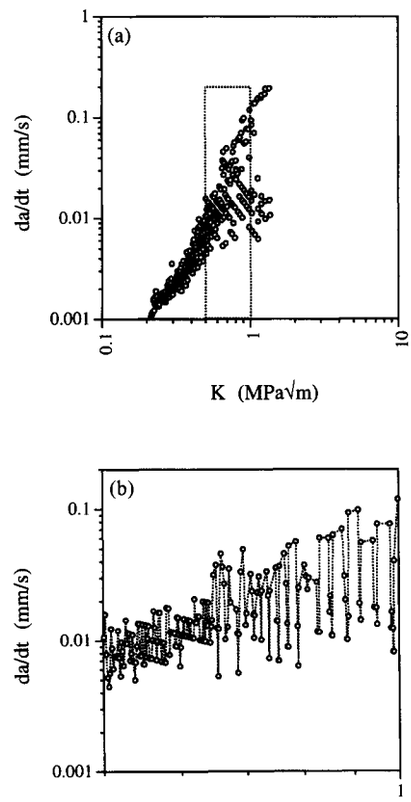

Figure 6 Crack growth rate *versus* stress intensity factor for PET in 1% caustic at: (a) full scale and (b) expanded scale

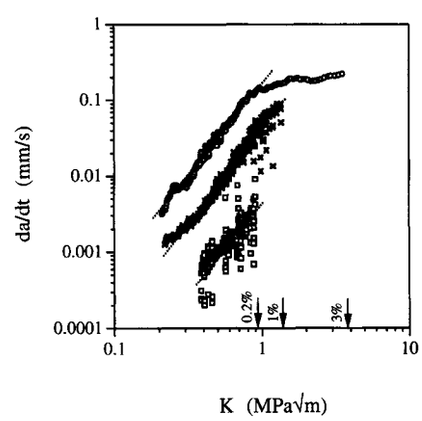

Figure 7 Effect of caustic concentration on crack growth in PET: (○) 3% caustic; (×) 1% caustic; (□) 0.2% caustic. Arrows indicate failure points

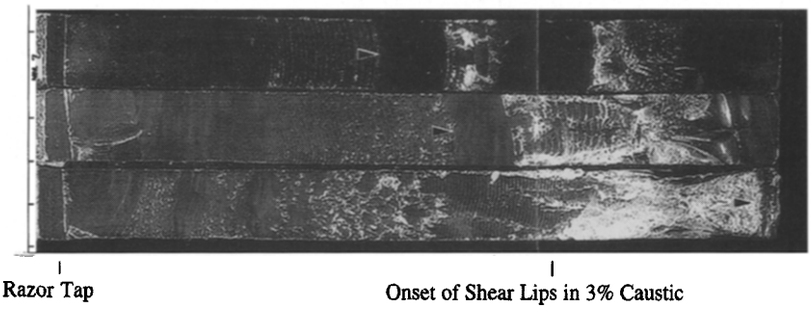

Figure 8 Optical micrographs of fracture surfaces of PET in 3% (bottom), 1% (middle), and 0.2% (top) caustic. Crack growth occurs from left to right

descending values of da/dt correspond to apparent crack growth from extension of the newly formed craze. The next high value of da/dt would occur when the crack jumps through the damaged craze zone, and so on.

The effect of caustic concentration on crack growth rate is illustrated in *Figure 7*. (Crack growth rates shown in *Figure 7* were determined by using a seven-point incremental polynomial method in order to minimize the apparent scatter in the plots and to aid in visualizing the effect of caustic concentration on da/dt.) As expected, da/dt at any given value of K increases as caustic concentration increases. Caustic concentration also influences the value of K at failure (K_c); K_c decreases with decreasing caustic concentration, as indicated by the arrows in *Figure 7*. An optical micrograph of the fracture surfaces of these specimens is shown in *Figure 8*. Arrowheads in *Figure 8* identify the onset of unstable crack propagation in each specimen. It is interesting to note that crack growth rate in the specimen exposed to 3% caustic reaches a plateau value of about 0.2 mm s^{-1} instead continuing to increase linearly with K. The plateau is a consequence of a transition in stress state at the crack tip from plane strain to plane stress and occurs as the crack tip approaches the back face of the compact tension specimen. The loss of constraint causes the crack tip to tunnel and shear lips to form on the fracture surface (see *Figure 8*). The value of K at which shear lips begin to form on the fracture surface corresponds closely to the onset of the plateau in da/dt for the specimen exposed to 3% caustic.

A close examination of the fractures surfaces in *Figure 8* reveals that the size of the discontinuous growth bands is a function of both the value of K and caustic concentration. A plot of band size *versus* crack length is shown in *Figure 9*. At a given crack length or value of K, band size decreases with increasing caustic concentration. At high caustic concentration, the craze at the tip of the crack does not have much time to grow before the craze zone is sufficiently damaged by hydrolysis to allow the crack to jump. At low caustic concentration, the craze can grow much longer before it is sufficiently weakened by hydrolysis. This is illustrated schematically in *Figure 10*. The longer jumps that occur in the dilute solutions may be responsible for the drop in K_c as caustic concentration decreases; long jumps are more difficult to stabilize than small jumps, resulting in premature failure in dilute caustic solutions.

Figure 9 also shows that for a given caustic concentration band size increases with increasing crack length, or value of K. Band size should be indicative of the length of the plastic zone ahead of the crack tip. According to Dugdale[11], the length of the crack tip plastic zone (r_p) is given by

$$r_p = \frac{\pi}{8}\left(\frac{K}{\sigma_y(t)}\right)^2 \tag{6}$$

where $\sigma^y(t)$ is a time-dependent yield stress. A trial-and-error method was used to determined the appropriate yield stress value to use in equation (6) in order to fit each set of data in *Figure 9*. Yield stress values of 31, 35 and 48 MPa were selected for the specimens tested in 0.2, 1 and 3%

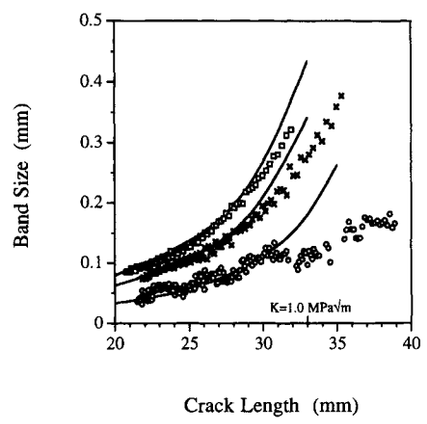

Figure 9 Effect of caustic concentration on size of discontinuous growth bands in PET. Symbols same as in *Figure 7*. Solid lines from equation (6)

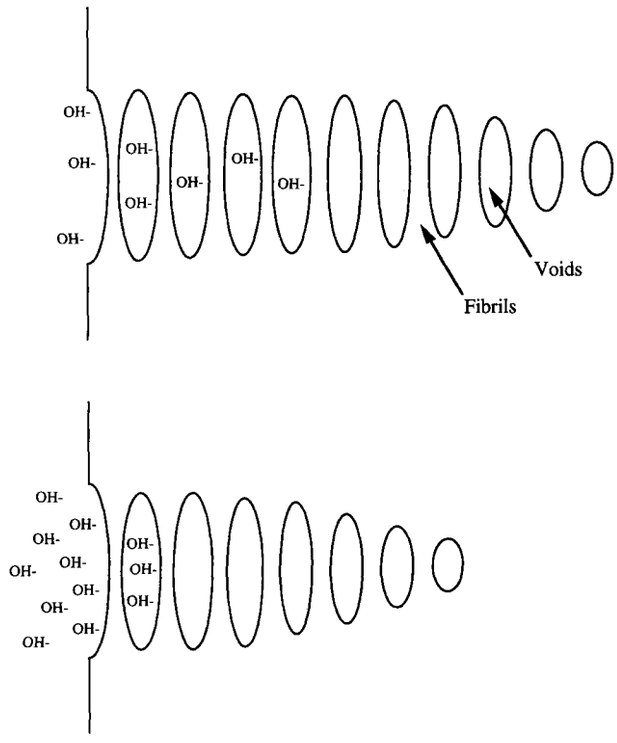

Figure 10 Schematic of caustic attack at low (top) and high (bottom) caustic concentrations

Table 1 Effect of caustic concentration on time to form discontinuous growth bands

Crack length (mm)	K (MPa$\sqrt{m}$)	Time to form discontinuous growth band (s)		
		3% Caustic	1% Caustic	0.2% Caustic
23	0.51	1.6	11.7	93.6
25	0.58	1.3	9.7	92.8
27	0.65	1.4	9.2	93.9
29	0.76	1.2	8.0	92.5
31	0.87	0.8	7.7	90.3
33	1.02	0.6	6.7	–
35	1.24	0.4	5.3	–

caustic, respectively. These yield stress values are reasonable considering that the yield stress for PET is 60.4 MPa as measured by ASTM Standard D638. Note that the effective yield stress increases with increasing caustic concentration since the time to form a band, and hence the time for craze formation, decreases with increasing caustic concentration. Band size for the specimen exposed to 3% caustic deviates substantially from predicted values above a crack length of about 30 mm due to the formation of shear lips as discussed above. Band size for specimens exposed to 0.2 and 1% caustic are modelled quite well by equation (6), although slight deviations occur in both specimens above a crack length of about 30 mm. This is probably due to the fact that the time to form a band, and hence the effective yield stress, changes slightly with increasing crack length, as shown in *Table 1*. Thus, in order to fit all band size data using equation (6), the yield stress would have to be gradually increased to reflect the change in the time available for band formation.

The time dependence of yield stress is often expressed by a power law of the form

$$\sigma_y(t) = \sigma_0 \left(\frac{t}{\tau_1} \right)^{-m} \tag{7}$$

where τ_1 is a time variable[12]. Equation (6) can now be recast as

$$r_p = \frac{\pi}{8} \frac{K^2}{\sigma_y} \left(\frac{t}{\tau_1} \right)^{2m} \tag{8}$$

Craze growth described by equation (8) is sometimes referred to as 'relaxation-controlled' growth because of the time dependence of the yield stress. The ability of equation (8) to model craze growth in this study is examined. A plot of crack length *versus* time for PET exposed to 0.1% caustic is shown in *Figure 11*. The stepwise nature of crack growth is accentuated in this specimen because of the low caustic concentration. An optical micrograph of the discontinuous growth band at a value of K of 1.12 MPa$\sqrt{m}$ and associated with the cluster of data highlighted in *Figure 11* is shown in *Figure 12*. Two distinct regions of craze growth are discernible within this band; an initial textured region which shows evidence of caustic

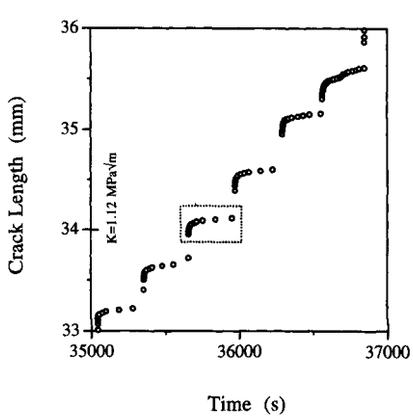

Figure 11 Crack length *versus* time for PET in 0.1% caustic

Figure 12 Optical micrograph of discontinuous growth bands in PET in 0.1% caustic. Crack growth occurs from left to right

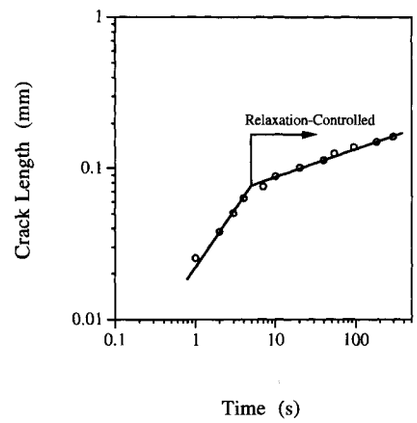

Figure 13 Craze growth curve for PET in 0.1% caustic

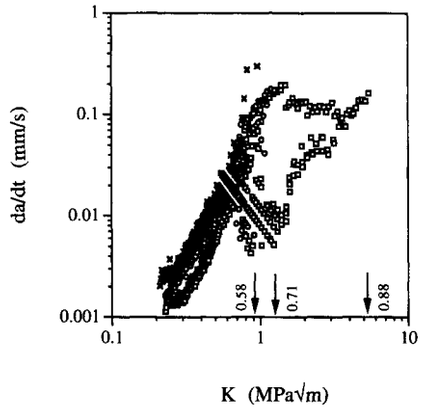

Figure 14 Effect of IV on crack growth in 1% caustic. Arrows indicate failure points

attack followed by a smoother, less featured region. A plot of log(crack length) *versus* log(time) for the band is shown in *Figure 13*. (It should be noted that the apparent crack length, and not craze length, is plotted in *Figure 13*. Recall that the change in apparent crack length ≈ craze length/2.) The data in *Figure 13* form two distinct lines, suggesting that two mechanisms of craze growth are operative, in agreement with observations from the fracture surface. The initial craze growth mechanism occurs over a very short period of time (< 5 s) and probably occurs when the crack jumps through the preceding craze and is forced to an abrupt stop by virgin material (see *Figure 4*). The caustic solution rapidly migrates into the newly formed craze and begins to hydrolyse the PET. Subsequent craze growth is relaxation-controlled with little accompanying diffusion of caustic.

The effect of PET resin IV on crack growth rate in 1% caustic is demonstrated in *Figure 14*. In the regime of stable crack growth common to all specimens ($K < 0.9$ MPa$\sqrt{m}$), d*a*/d*t* at a given value of K decreases only slightly with increasing IV. However, the value of K_c and consequently the lifetime of the specimen increase substantially with increasing IV. This suggests that the ability of the polymer to arrest a growing crack and form a stable craze according to the mechanism described in *Figure 4* depends on its molecular weight. Analogous results have been reported by Fellers and Kee who showed that the stress required to initiate a craze is independent of polymer molecular weight, but that the stress required to fracture a craze increases with molecular weight[13].

CONCLUSIONS

A fracture mechanics approach was used to evaluate environmental stress cracking of amorphous PET in aqueous sodium hydroxide. Crack growth rate increased with increasing stress intensity factor and caustic concentration. PET resin molecular weight had only a slight effect on crack growth rate in the regime of stable crack propagation, but significantly influenced the critical stress intensity factor. Crack growth occurred by the formation of discontinuous growth bands. Band size was a function of stress intensity factor and caustic concentration and could be modelled by the Dugdale plastic zone. Fractographic analysis showed that each band comprised two distinct stages of craze growth, with caustic attack being evident only in the initial stage.

ACKNOWLEDGEMENTS

The author thanks Earl Newman for designing the creep rig, Mona Jank for assisting with the experimental work, and Doctors Thomas Pecorini and Terrill McGee for many helpful discussions.

REFERENCES

1. Kambour, R.P., *Macromolecular Review*, 1973, **7**, 1.
2. Kramer, E.J., in *Developments in Polymer Fracture*, Vol. 1, ed. E.H. Andrews. Applied Science, London, 1979, Ch. 3.
3. Volynskii, A.L. and Bakeev, N.F., *Solvent Crazing of Polymers*. Elsevier, Amsterdam, 1995.
4. Wright, D.C., *Environmmental Stress Cracking of Plastics*. Rapra Technology Limited, Shawbury, UK, 1996.
5. Zeronain, S.H., Wang, H.Z. and Aiger, K.W., *Journal of Applied Polymer Science*, 1990, **41**, 527.
6. Moskala, E.J., in *Conference Procedings of BEV-PAK AMERICAS'96*, Fort Lauderdale, FL, April, 1996.
7. Beaumont, P.W.R. and Young, R.J.J., *Material Science*, 1975, **10**, 1334.
8. Saxena, A. and Hudak, S.J., *International Journal of Fracture*, 1978, **14**, 453.
9. Kinloch, A.J. and Young, R.J., *Fracture Behavior of Polymers*. Elsevier, Oxford, 1988.
10. Lu, X., Qian, R. and Brown, N.J., *Material Science*, 1991, **26**, 917.
11. Dugdale, D.S., *Journal of Mechanics, Physics and Solids*, 1960, **8**, 100.
12. Williams, J.G., *Fracture Mechanics of Polymers*. Ellis Horwood, Chichester, 1987.
13. Fellers, J.F. and Kee, B.F., *Journal of Applied Polymer Science*, 1974, **18**, 2355.